12th International Conference on Advances in Steel-Concrete Composite Structures (ASCCS 2018)
Universitat Politècnica de València, València, Spain, June 27-29, 2018
Doi: http://dx.doi.org/10.4995/ASCCS2018.2018.7060

Design for Deconstruction for Sustainable Composite Steel-Concrete Floor Systems

L. Wang[a], M. D. Webster[b] and J. F. Hajjar[a]*

[a]Department of Civil and Environmental Engineering, Northeastern University, Boston, USA
[b]Simpson Gumpertz & Heger Inc., Waltham, USA
*corresponding author, e-mail address: JF.Hajjar@northeastern.edu

Abstract

Conventional steel-concrete composite floor systems utilizing steel headed stud anchors and metal decks are cost-effective and widely used solutions for non-residential multi-story buildings, due in part to their enhanced strength and stiffness relative to non-composite systems. Because these systems use steel headed stud anchors welded onto steel flanges and encased in cast-in-place concrete slabs to achieve composite action, it is not possible to readily deconstruct and reuse the steel beams and concrete slabs. As the building industry is moving towards sustainability, there are clear needs for developing sustainable steel-concrete composite floor systems to facilitate material reuse, minimize consumption of raw materials, and reduce end-of-life building waste. This paper presents the behavior and design strategies for a sustainable steel-concrete composite floor system. In this system, deconstructable clamping connectors are utilized to attach precast concrete planks to steel beams to achieve composite action. The load-slip behavior of the clamping connectors was studied in pushout tests, and the test results showed that the clamping connectors possess similar shear strength to 19 mm diameter shear studs and much greater slip capacity. Four full-scale beam tests were performed to investigate the flexural behavior of the deconstructable composite beams under gravity loading and validate the connector behavior attained from the pushout tests. All the beams behaved in a ductile manner. The flexural strengths of the composite beam specimens closely match the strengths predicted for composite beams by the design provisions of the American Institute of Steel Construction (AISC).

Keywords: *Design for Deconstruction; composite floor system; clamping connector; pushout test; composite beam test.*

1. Introduction

Steel-concrete composite floor systems offer excellent advantages over non-composite floor systems, including enhanced flexural strength and stiffness, reduced steel beam size and depth, and increased economy. In current construction practice, steel headed stud anchors are welded through metal decks onto steel flanges and embedded in cast-in-place concrete slabs to achieve composite action, resulting in a highly efficient, but integrated design. After demolition, the steel beams and shear studs in the conventional composite floor systems generally are extracted from the demolition debris and recycled, while the concrete slabs may be broken up and sent to landfills or crushed to make aggregate for fill or new concrete.

In this paper, a new sustainable steel-concrete composite floor system, which consists of precast concrete planks attached to steel beams via clamping connectors, is proposed to facilitate material reuse, minimize consumption of raw materials, and reduce end-of-life building waste. A comprehensive experimental investigation of the system is described, and the pushout test results and beam test results demonstrate the load-slip behavior of the clamping connectors and the load-deflection performance of the deconstructable composite beams, respectively. Design recommendations are also given to predict the elastic stiffness and flexural strengths

of similar deconstructable composite beams using clamping connectors.

2. Experimental program

A new deconstructable composite beam prototype is illustrated in Fig. 1; the original concept was first introduced in Webster et al. [1]. In the system, precast concrete planks are attached to steel beams using clamping connectors. High strength T-bolts, which are inserted in cast-in channels, are pretensioned to firmly clamp the top steel flange to the underside of the concrete plank. The resulting friction generated at the steel-concrete interface is utilized to achieve composite action in the composite beams.

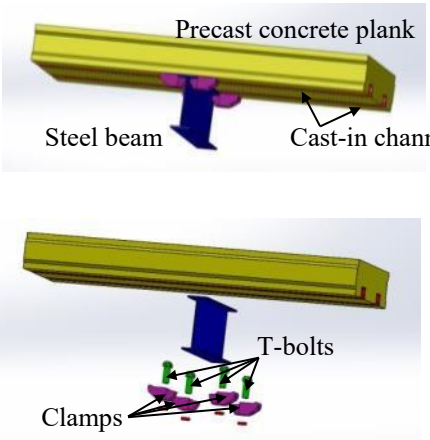

Fig. 1. Deconstructable composite beam prototype.

The following sections summarize the testing program and experimental results to demonstrate the behavior of the proposed system. Refer to Wang [2] for more details.

2.1. Pushout tests

2.1.1 Pretension tests

To ensure that reliable normal force and friction are generated between the steel beams and concrete planks in the system, it is desirable to yield the bolt material after pretensioning. Since the heads of the T-bolts and the lips of the channels which the T-bolts are inserted into are both deformable, the required nut rotations established for standard bolted connections given in Table 8.2 in the RCSC Specification (2014) [3] are no longer applicable. Thus, prior to pushout tests, pretension tests, which simulate actual assembly conditions, were performed to determine the number of turns of the nut to pretension the T-bolts.

In the pretension test setup shown in Fig. 2, three bolts were snug-tightened to restrain the movement of the steel beam, and the nut of the fourth bolt was rotated until fracture occurred in the bolt head or shank. Three M24 and M20 bolts were tested. As shown in Fig. 3, with the exception of one M24 bolt whose head fractured, all the bolts ultimately fractured in their shanks. Prior to fracture, the ultimate nut rotation was at least 4 complete turns for all six bolts.

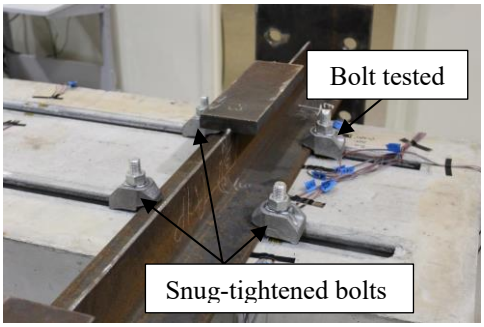

Fig. 2. Pretension test setup.

M24 bolts M20 bolts

Fig. 3. Fractured bolts.

During testing, the axial strain variation of each bolt was measured using two uniaxial strain gages that were attached on the bolt shank after removing the threads locally. Using the stress-strain curve obtained from tensile coupon testing for the bolt material, stress-strain relationships were plotted for typical M24 and M20 bolts in Fig. 4. The stress and strain at every half turn after a snug-tight condition are also identified on the curves.

Based on the stress-strain relationships of all six bolts, 2 turns and 1.5 turns after a snug-tight condition are recommended for pretensioning the M24 bolts and M20 bolts, respectively, since the stress-strain relationships plateau at these rotations, indicating that the bolt material has yielded, and any moderate strain variation leads to a minor change in the bolt tension.

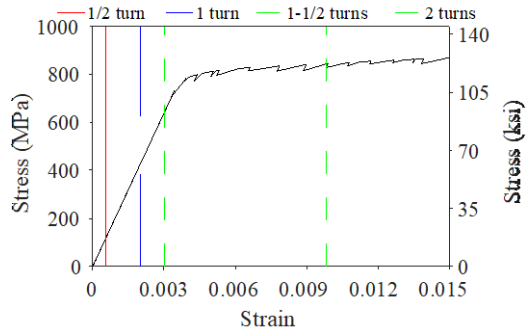

a) M24 bolt

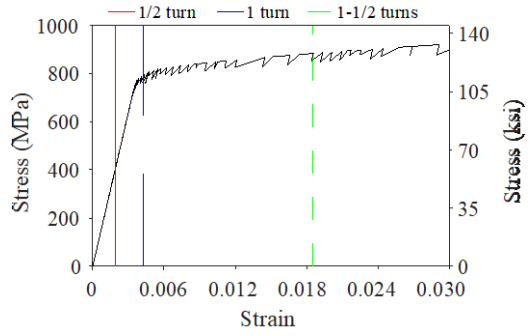

b) M20 bolt

Fig. 4. Bolt axial stress-strain relationship in pretension tests.

2.1.2 Pushout tests

The pushout test setup is illustrated in Fig. 5. The pushout specimen consisted of a 1219 mm by 610 mm by 152 mm (4 ft. × 2 ft. × 6 in.) concrete plank attached to a WT5×30 or WT4×15.5 section using M24 or M20 clamps. To view the motion of the clamps and steel beam, the pushout specimen was mounted upside down. The slip at each clamp was measured using a linear potentiometer.

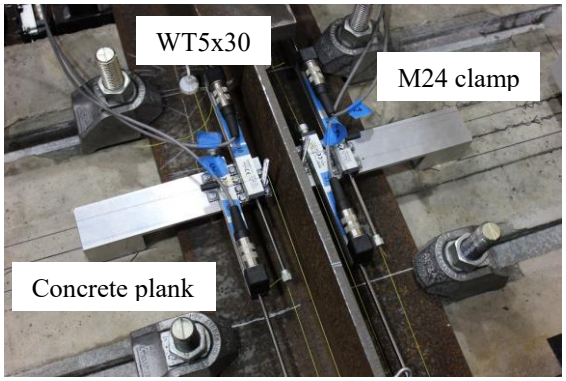

Fig. 5. Pushout test setup.

The pushout test matrix is shown in Table 1. The test parameters include: (1) loading protocol: the clamping connectors were tested under monotonic and cyclic loading to mimic applications in composite beams and composite diaphragms, respectively; (2) bolt diameter: both M24 and M20 bolts were tested; (3) number of cast-in channels: two-channel planks were considered standard specimens; however, heavy gravity loading may necessitate three-channel specimens to attain larger flexural strength than two-channel specimens; (4) reinforcement configuration: the light reinforcement pattern, which was designed for gravity loading only, was utilized in one cyclic specimen to explore anchor-related concrete failure modes, while the heavy reinforcement configuration, which contained additional supplementary reinforcement placed around the channel anchors, was adopted for the remaining specimens to ensure that the limit state is slip of the clamps; (4) shim: steel plates were inserted between the clamp teeth and steel flanges in two specimens to enable the M24 clamps to be tested with the WT4×15.5 sections.

Table 1. Pushout test matrix

Specimen	Test parameters			
	Bolt size	# of channels	Rebar	Shim
1-m24-c2-h	M24	2	Heavy	No
2-m24-c2-hs	M24	2	Heavy	Yes
3-m24-c3-h	M24	3	Heavy	No
4-m20-c2-h	M20	2	Heavy	No
5-c24-c2-h	M24	2	Heavy	No
6-c24-c2-l	M24	2	Light	No
7-c24-c2-hs	M24	2	Heavy	Yes
8-c24-c3-h	M24	3	Heavy	No
9-c20-c2-h	M20	2	Heavy	No

The load-slip curves of the monotonically loaded pushout specimens are illustrated in Fig. 6. Testing of all the monotonic specimens was terminated due to excessive slip of the clamps, and no specific limit states were observed.

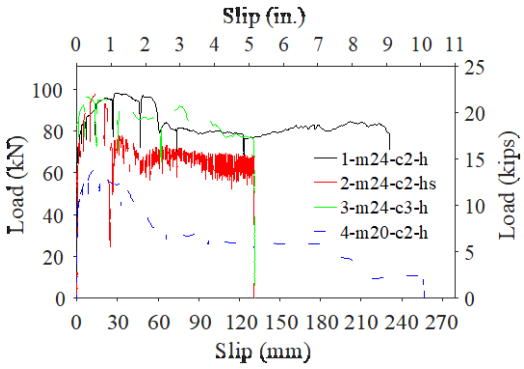

Fig. 6. Load-slip curves of monotonic pushout specimens (per connector).

The behavior of specimens 1-m24-c2-h and 3-m24-c3-h is very ductile throughout the tests, and the strength degradation is less than 20% even at a slip of 127 mm (5 in.). Three complete turns of the nut was initially applied to pretension the bolts in specimens 1-m24-c2-h and 2-m24-c2-hs. However, the head of one of the bolts in specimen 2-m24-c2-hs fractured during the test, as indicated by the sharp strength reduction at a slip slightly less than 25.4 mm (1 in.). Shortly after the fracture, load oscillation began which could be attributed to a stick-slip mechanism exacerbated by the shims. It is also seen that use of the shims neither reduces the peak strength of the specimen nor affects the behavior of the specimen until bolt fracture.

As indicated by the load-slip curve of specimen 4-m20-c2-h, the strength of the specimen gradually declines starting at a slip of 17.3 mm (0.68 in.), which results from the bolt tension reduction induced by the large rotation of the clamps, as shown in Fig. 7. This is due to the channel lips (which are the same size for all tests) not being adequately large to support the M20 clamps as fully as the M24 clamps are supported, or due to the contact of the clamp teeth with the steel flange having too small an area compared to the M24 clamp. Redesigning the M20 clamps, e.g., interlocking the clamp tail into the channel to restrain its rotation, and utilizing appropriately sized channels may mitigate the strength degradation of the smaller clamps at large slips.

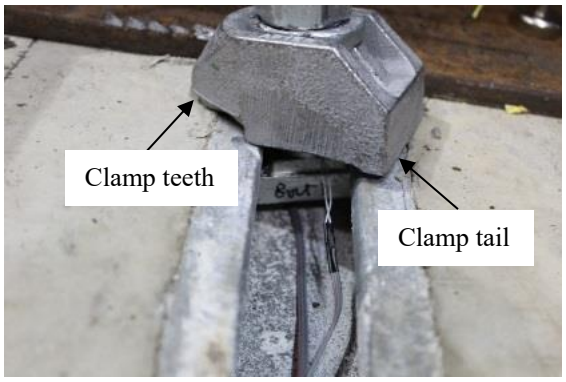

Fig. 7. Large rotation of M20 clamps.

If used in composite beams, the behavior of the clamps in the monotonic specimens at slips comparable to those seen in deconstructable composite beams is of particular interest. These slips should be obtained from the composite beam tests discussed in the next section. As documented in Wang [2], the slip at the serviceability of the beam specimens ranged from almost zero to 1.27 mm (0.05 in.), and the ultimate slip varied from 0.51 mm (0.02 in.) to 8.89 mm (0.35 in.). At the serviceable slip, the behavior of the clamps in the beam specimens was very likely to resemble the initial and very stiff portions of the load-slip curves presented in Fig 6. At the ultimate slip, the clamps in the beam specimens probably approached their peak strength, and no strength degradation was anticipated.

The load-slip curves of specimens 5-c24-c2-h and 6-c24-c2-l are plotted in Fig. 8. Testing of these two specimens was terminated due to excessive slip of the clamps, and no specific limit states were observed.

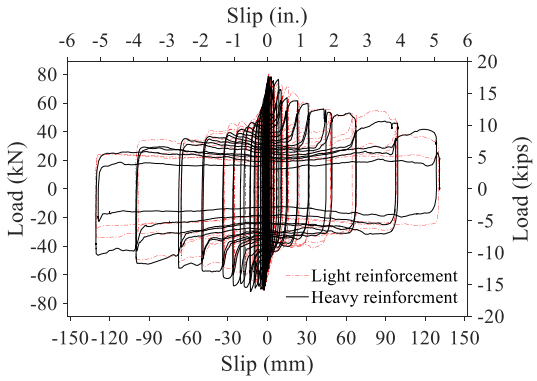

a) Overall behavior

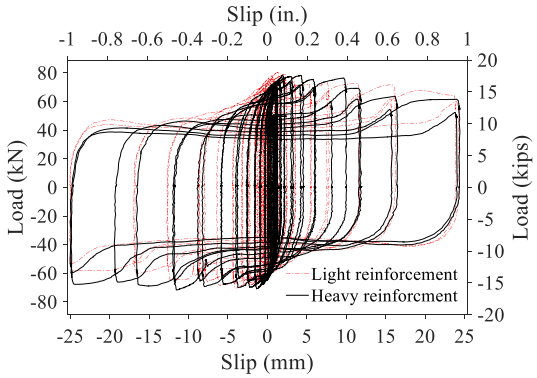

b) Behavior within 25.4 mm slip

Fig. 8. Load-slip curves of cyclic pushout specimens (per connector).

The overall behavior of the two specimens is shown in Fig. 8a. Similar to that observed for shear studs [4], the peak strength and ductility of the cyclic specimens are reduced, compared to the corresponding monotonic specimen (i.e., specimen 1-m24-c2-h). This is due to the reduction of the frictional coefficients at the slip planes, which is caused by smoothing of the contact surfaces during cycling, and the release of the bolt pretension, which is caused by the

damage to the steel flanges and clamp teeth. In design, the cyclic shear strengths of the clamps could be calculated as 80% of their monotonic shear strengths. This coefficient is determined as the mean of the ratios of the peak strengths of the cyclic specimens to the peak strengths of the corresponding monotonic specimens [2].

If used in composite diaphragms to transfer in-plane inertia forces to lateral force-resisting systems, the behavior of the clamps in the cyclic specimens should be evaluated within typical slip demand ranges, which are conservatively assumed to be +/-25.4 mm (1 in.) slip. As depicted in Fig. 8b, the behavior of the two specimens is excellent within this range. The insignificant differences between the two curves in Fig. 8 indicate that the elimination of the additional supplementary reinforcement in the light reinforcement configuration had negligible impacts on the behavior of the pushout specimens.

2.2. Beam tests

The beam test setup is shown in Fig. 9. Each beam specimen consisted of a 9144 mm (30 ft.) long steel beam connected with fifteen 2438 mm by 610 mm by 152 mm (8 ft. × 2 ft. × 6 in.) concrete planks using clamping connectors. The loading on the specimens was spread using spreader beams to approximate uniform loading supported by secondary beams in a structure. A pin support and a roller support were placed at the beam ends to simulate simply-supported boundaries.

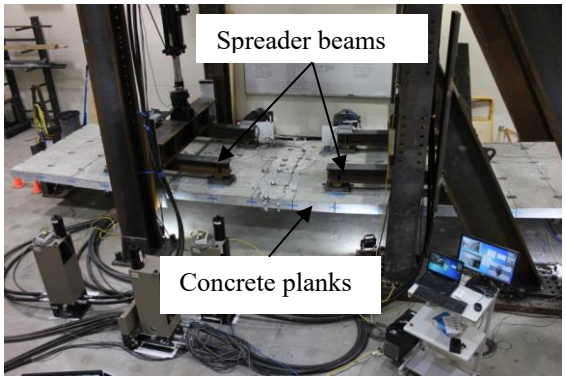

Fig. 9. Beam test setup.

The beam test matrix is shown in Table 2. Two W14×38 and W14×26 sections were tested with the M24 and M20 clamps, respectively. As the most important test parameter, the percentage of composite action of the specimens ranged from more than 100% to approximately 44%.

The load-center deflection curves of the deconstructable composite beam specimens are illustrated in Fig. 10. All the specimens were first loaded to 40% of their predicted flexural strengths, unloaded and then reloaded three times. Two more loading/unloading cycles were then applied to the specimens, with one cycle at 60% and the other one at 80% of the expected flexural strengths of the specimens. These cycles were intended to mimic serviceability conditions. After completing these cycles, the specimens were loaded until the beams almost touched the concrete strong floor.

Table 2. Beam test matrix

Specimen	Test parameters			
	Bolt size	# of channels	Rebar	% of composite action
1-m24-c2	M24	2	Heavy	82.7%
2-m24-c1	M24	1	Light	45.1%
3-m20-c3	M20	3	Light	137.8%
4-m20-c1	M20	1	Light	43.8%

All the load-center deflection curves are shifted from the origins to account for the bending moment and deflection generated due to the self-weight of the beam specimens after removing the shoring used during construction. All the beams exhibited ductile behavior, and little or no strength reduction is observed from the load-center deflection curves, even though the beams were ultimately deflected to approximately $L/25$.

Major events are identified on the curves, including slip of the clamps, yielding of the steel beam, localized concrete crushing and first bang heard during the tests. Although the design of the specimens is not governed by the compressive strength of the concrete planks, localized concrete crushing occurred along the top edges of the planks, as shown in Fig. 11.

Table 3 summarizes the key results from the composite beam tests. The stiffness calculated using a lower bound moment of inertia (I_{LB} from AISC (2016a) [5]) underestimates the tested stiffness of the deconstructable composite beam specimens. As the percentage of composite action increases, the stiffness of the composite beams increases, as is indicated by the comparison between specimen 1-m24-c2 and

specimen 2-m24-c1 and between specimen 3-m20-c3 and specimen 4-m20-c1.

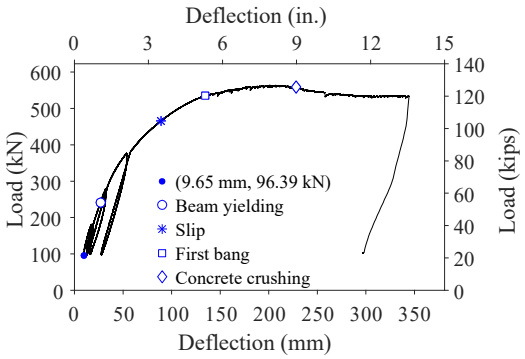

a) Specimen 1-m24-c2

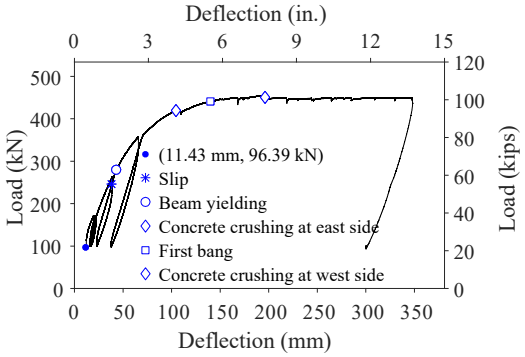

b) Specimen 2-m24-c1

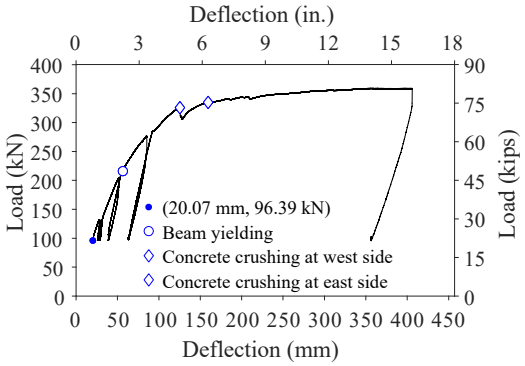

c) Specimen 3-m20-c3

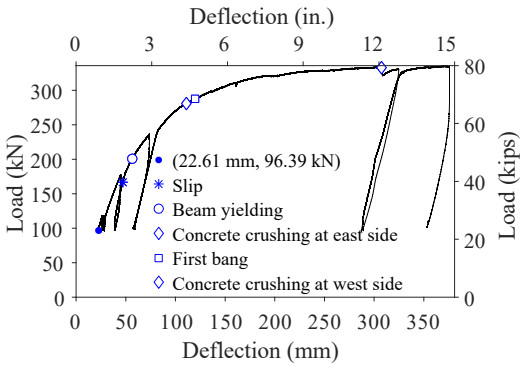

d) Specimen 4-m20-c1

Fig. 10. Load-center deflection curves of deconstructable composite beam specimens.

Fig. 11. Localized concrete crushing in specimen 2-m24-c1 at 190 mm deflection.

With the exception of specimen 4-m20-c1, the experimental flexural strengths of the beam specimens are close to those predicted by AISC (2016a) [5], which probably indicates that the ultimate flexural strengths of the specimens are not affected by the localized concrete crushing shown in Fig. 11.

Table 3 indicates that the maximum slip of the clamps is inversely proportional to the amount of composite action of the specimens, with the smallest and largest slip occurring in beams with the highest and lowest levels of composite action, respectively.

After testing, all the specimens were disassembled by loosening the bolts, and a deconstructed steel beam is shown in Fig. 12. In typical applications where a beam would not be subjected to ultimate loads, it is anticipated the steel beam would be in its elastic state when deconstructed.

Fig. 12. Deconstructed steel beam from specimen 1-m24-c2.

Table 3. Beam test results.

Specimen	Stiffness kN/mm (kips/in.)			Flexural strength kN-m (ft.-kips)			Maximum slip mm (in.)	
	Test	AISC	Test/AISC	Test	AISC	Test/AISC	West side	East side
1-m24-c2	9.24 (52.8)	8.67 (49.5)	1.07	777 (571)	769 (565)	1.01	5.94 (0.234)	6.43 (0.253)
2-m24-c1	7.76 (44.3)	6.81 (38.9)	1.14	634 (469)	632 (466)	1.01	8.18 (0.322)	6.45 (0.254)
3-m20-c3	6.46 (36.9)	6.10 (34.8)	1.06	494 (364)	510 (376)	0.97	0.46 (0.018)	0.23 (0.009)
4-m20-c1	6.08 (34.7)	4.43 (25.3)	1.37	476 (351)	401 (296)	1.19	8.79 (0.346)	8.08 (0.318)

3. Conclusions

A new deconstructable composite floor system, which consists of precast concrete planks attached to steel beams via clamping connectors, is proposed to facilitate material reuse, minimize consumption of raw materials, and reduce end-of-life building waste.

Based on the experimental and corroborating computational results, the following conclusions are reached for the behavior of the deconstructable composite floor system:

(1) Based on the pretension test results, 2 turns and 1.5 turns after a snug-tight condition are recommended for pretensioning the M24 bolts and M20 bolts, respectively.

(2) The behavior of the clamps in all the pushout specimens is excellent at typical slip demands expected in deconstructable composite beams and composite diaphragms, demonstrating the potential of using the clamping connectors in these applications.

(3) At a slip of 127 mm (5 in.), the monotonic specimens using the M24 clamps retained approximately 80% of their peak strengths. In contrast, as the slip increased, the strength of the monotonic specimen using the M20 clamps declined. However, if used in applications where the slip is large, the M20 clamps could be redesigned, e.g., interlocking the clamp tail into the channel to restrain its rotation, or utilized with appropriately sized channels to mitigate this issue.

(4) Although load oscillation, which could be induced by a stick-slip mechanism, was seen in the pushout specimens using shims between the steel flanges and clamps, neither the peak strength nor the load-slip behavior of the specimens were affected by the shims at slips comparable to those seen in deconstructable composite beams, which were less than 8.89 mm (0.35 in.) even at peak deflections well past service load deflections.

(5) Because the abrasion between the steel flange and the clamp teeth and between the steel flange and the concrete plank in the early cycles smoothed the slip planes and released some of the bolt tension, the strengths of the cyclic pushout specimens were lower than the corresponding monotonic pushout specimens, which could be accounted for in design using a strength reduction coefficient of 0.8. If needed for withstanding large slips, the clamp teeth may be reconfigured to minimize the damage to the steel flange and clamp teeth, thus maintaining the bolt tension throughout the test.

(6) Four full-scale deconstructable composite beams with different levels of composite actions were tested. All the specimens were ultimately deflected to approximately $L/25$, and the beams behaved in a ductile manner with little or no strength degradation observed, even though localized concrete crushing occurred along the top edges of the concrete planks at very large deflections.

(7) The stiffness of the deconstructable composite beams can be conservatively estimated with a lower bound moment of inertia given in AISC 360-16. The flexural strengths of the beams closely match those predicted by the AISC provisions.

The channel, T-bolt, and clamp are commercially available components. The

components were not originally designed by the manufacturers to work together in the proposed configuration, which resulted in certain behavior limitations that could be addressed by the development of modified components tailored to this particular application.

Acknowledgments

This material is based upon work supported by the National Science Foundation under Grants No. CMMI-1200820 and No. IIS-1328816, the American Institute of Steel Construction, Northeastern University, and Simpson Gumpertz & Heger. In-kind support is provided by Benevento Companies, Capone Iron Corporation, Fastenal, Halfen, Lehigh Cement Company, Lindapter, Meadow Burke, Souza Concrete, and S&F Concrete. This support is gratefully acknowledged. The authors would like to thank Kyle Coleman, Michael McNeil, Kurt Braun, Corinne Bowers, Edward Myers, Majed Alnaji, Michael Bangert-Drowns, Kara Peterman, Angelina Jay, Justin Kordas, David Padilla-Llano, and Yujie Yan for their assistance with the experiments. Any opinions, findings, and conclusions expressed in this material are those of the authors and do not necessarily reflect the views of the National Science Foundation or other sponsors.

References

[1] Webster M, Kestner D, Parker J, Johnson M. Deconstructable and Reusable Composite Slab. Winners in the Building Category: Component – Professional Unbuilt, Lifecycle Building Challenge; 2007 <http://www.lifecyclebuilding.org/2007.php>

[2] Wang L. Deconstructable Systems for Sustainable Design of Steel and Composite Structures. Ph.D. Dissertation, Department of Civil and Environmental Engineering, Northeastern University, Boston, USA; 2017.

[3] RCSC. Specification for Structural Joints Using High-Strength Bolts. Research Council on Structural Connections, Chicago, Illinois; 2014.

[4] Pallarés L, Hajjar JF. Headed Steel Stud Anchors in Composite Structures: Part I. Shear. Report No. NSEL-013, Newmark Structural Laboratory Report Series (ISSN 1940-9826). Department of Civil and Environmental Engineering, University of Illinois at Urbana-Champaign, Urbana, Illinois, April 2009.

[5] AISC. Specification for Structural Steel Buildings, American Institute of Steel Construction, Chicago, Illinois; 2016.